

# Quantitative Measurement of Deformational Plagiocephaly and Brachycephaly at the Point-of-care

**Reza Seifabadi, PhD, Fereshteh Alamifar, PhD, S. Hossein Hezaveh, PhD, Can Kocabalkanli, MSc, and Marius George Linguraru, DPhil**

PediaMetrix Inc., 155 Gibbs St., Suite 537, Rockville, MD, USA, 20850

## ABSTRACT

**Purpose:** to develop and validate algorithms that enable a novice user to quantitatively measure the head shape parameters associated with deformational plagiocephaly, and brachycephaly (DPB) using a smartphone or tablet.

**Method:** We have developed a technology (called *SoftSpot*<sup>TM</sup>) based on advanced imaging algorithms to detect different types and severity of DPB from top-view photos of the head acquired by a novice user at the point-of-care, i.e. in pediatric offices, and at home. Currently, the head shape parameters are measured using either a 3D scanner or a mechanical caliper by a specialist such a pediatric neurosurgeon or an orthotist. In our approach, the head contour is extracted semi-automatically using the intelligent scissors method. We then automatically compute two indices used in the clinical determination of the DPB: the cranial index (*CI*), and the cranial vault asymmetry index (*CVAI*). In this paper, we also present methods to quantify, and compensate for the user variability in the acquisition of photos, including camera angle, and distance from the head, by combining the results from different camera positions. We compared the results of our technology with ground truth measurements from 53 infants with DPB, and normal cranial parameters. Accuracy analysis was performed by Bland Altman (BA) method, and the Spearman correlation test.

**Results:** The Spearman correlation coefficients between the new 2D method, and the 3D ground truth were 0.94 ( $p<0.001$ ), and 0.96 ( $p<0.001$ ) for *CI* and *CVAI*, respectively. Different camera angles, and distances from the head resulted in variation in *CI* and *CVAI* in the range of [-2.0, 6.0], and [-4.0, 4.0] units, respectively. The limit of agreement was reduced from [-3.6, 5.3], and [-3.6, 4.2] to [-0.5, 3.0], and [-1.3, 1.6] for *CI* and *CVAI*, respectively, by combining results from different camera angles, and positions in our method. The overall accuracy of the proposed technology for DPB detection was 100%.

**Conclusions:** Photographic 2D images can be accurately analyzed to assess DPB at the point-of-care. By compensating for the error from variable camera angles, and distance from the head, our technology eliminates user variability. The algorithms will be packaged in a mobile application to enable the use of the technology at the point-of-care.

**Keywords:** Deformational plagiocephaly and brachycephaly (DPB), point-of-care, smartphone, early detection, quantitative measurement

## 1. INTRODUCTION

About 20-30% of newborns manifest moderate to severe head deformation in the first months after birth [1], and delayed identification causes significant medical and societal costs. The most common infant head deformations are deformational plagiocephaly and brachycephaly (DPB), see Figure 1.a. These conditions require immediate attention, and benefit from early treatment. Abnormal head shape or growth patterns in infants are correlated with other health conditions such as developmental delays, torticollis, microcephaly, and hydrocephalus [1,2-11]. In addition, these children and their families are affected by social stigma and psychological pressure. Therefore, it is essential to monitor the growth of infant heads to be able to initiate early, and less invasive therapy for children with head deformation, i.e., to prevent the need for helmet therapy for DPB, and associated health complications [12-16].

The incidence of DPB has risen from 2-5% to 20-46% since the Back-to-Sleep campaign was initiated [1,17] to avoid sudden infant death syndrome, causing DPB to be called a pediatric epidemic [18]. For diagnosis, families are referred by a pediatrician to orthotists or pediatric neurosurgeons who use a mechanical caliper called craniometer [19] (Figure 1.b) or 3D imaging [20] to determine the type and severity of the cranial deformation. It can take up to two months to schedule such visits, leaving parents in anxiety, and potentially missing the opportunity to correct DPB by conservative therapy [17], which is effective only in the first 4-6 months of life.

A critical challenge in the early detection of cranial deformations is the absence of tools available to pediatricians to perform quantitative head shape assessment during brief well-child visits. Typically, only the head circumference of the infant is measured using a tape. Moreover, head shape evaluation performed by specialists is done only for the indication of cranial deformation. As a result, over 600,000 infants remain untreated every year in the U.S for their head deformations [18]. Thus, there is a critical need to develop, and disseminate objective tools for simple, low cost, and reproducible assessment of cranial shape in pediatrician offices.

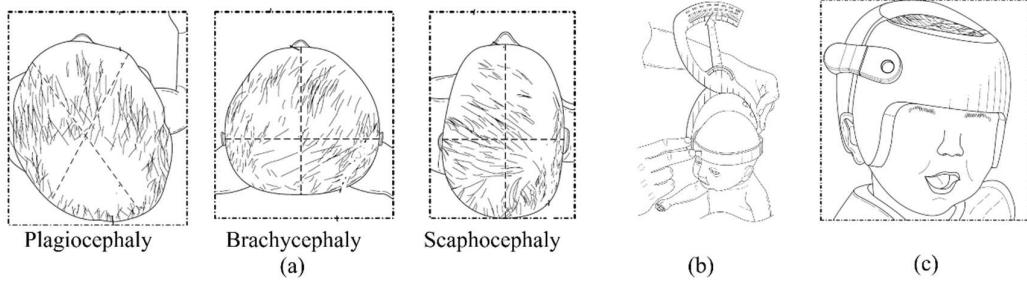


**Figure 1.** Measurement and management of DPB: a) types of DPB: plagioccephaly--when the head is asymmetric, brachycephaly--when the head is wider than normal, and scaphocephaly--when the head is longer than normal; b) craniometer to measure DPB by a specialist; c) correctional helmet for treatment of DPB.

In this paper, we first present algorithms that enable the semi-automatic measurement of the head shape parameters associated with DPB from top-view 2D rendered images of the head. We also simulate the effect of user variability in the acquisition of data, such as the camera angle and distance from the head, and landmark selection (the tip of the nose) on the accuracy of the cranial shape parameters. Then, we propose methods to compensate for the user variability error. Finally, we report the accuracy of our technology using 2D rendered images of infants with DPB and normal cranial shape.

## 2. METHODS

We have developed a technology (called *SoftSpot*) based on advanced imaging algorithms to detect different types and severity of DPB from top-view photos of the head acquired by a novice user at the point-of-care, i.e. in pediatric offices and at home. We aim to automatically compute two indices used in the clinical determination of the DPB from the head shape parameters: the cranial index (*CI*) and the cranial vault asymmetry index (*CVAI*) [21].

**Measurement of *CI* and *CVAI* from 2D photographs in the absence of user variability error.** We used 53 retrospective, curated 3D data from patients with normal head shape or DPB (both plagioccephaly/brachycephaly and scaphocephaly). The dataset was acquired using 3dMDHead System (3dMD, Atlanta, GA) or STARscanner (Orthomerica, Orlando, FL). The ground-truth *CI* and *CVAI* was obtained from the 3D scans of the head. Our measurements were performed on 2D pictures of the head.

Accurate extraction of the head contour is a prerequisite to measuring *CI* and *CVAI*. In our initial approach, the user clicks 6-10 points that roughly trace the head contour on the picture. Then, the contour is refined using the intelligent scissors algorithm in which a graph is constructed from the image using the seeds. Then the Dijkstra algorithm [24] is used to find the optimal path between consecutive seed points [25], which is smoothed using a piecewise cubic spline. Given the head contour, the *CI* and *CVAI* are calculated using a published method [21]. In that study, human experts manually identified landmarks for the measurement of *CI* and *CVAI*. In our methods, the identification of the landmarks is automatic.

Results were evaluated using Bland-Altman (BA) analysis and Spearman correlation test. The overall accuracy, sensitivity and specificity of our method for the identification of DPB were also measured and reported.

**Quantify and compensate for the effect of user variability on *CI* and *CVAI* measurements.** The notion of apparent contour can best describe the effect of camera angle and distance on *CI* and *CVAI* measurements. Apparent contours are the projection of the contour generators, as shown in Figure 2, for a given angle and distance from the target (i.e., the head), which separate the visible and occluded parts on a surface [26]. In other words, the apparent contour is what appears in the photo, and is a function of the ground-truth contour, as well as of the camera angle, camera-to-head distance, and camera parameters. The measurement plane is a plane that parallels to the XY plane at the level of the

largest head circumference. The XY plane is defined based on certain anatomical landmarks, i.e., the left and right tragi, nasion, and subnasale.

Through simulations, we generated top-view 2D projections of the head from the 3D head volumes to study the effect of camera angle and distance on the accuracy of cranial shape parameters. Two angles were defined for the relative pose of the smartphone to simulate the effect of variable input by novice users. Pitch and roll were varied from  $-6^\circ$  to  $14^\circ$  and  $-8^\circ$  to  $8^\circ$ , respectively. The camera distance was set at 300, 400, and 500 mm from the head. In total, 507 2D projections were generated from every 3D volume. Next, the head contour was automatically extracted from the 2D pictures.

To perform this automatic extraction, the nose and ears were removed through a series of morphological operations. Figure 3 shows an example image that contains the ears and nose tip, the output/processed image, and the difference between the two. We then computed the *CI* and *CVAI* from top view pictures.

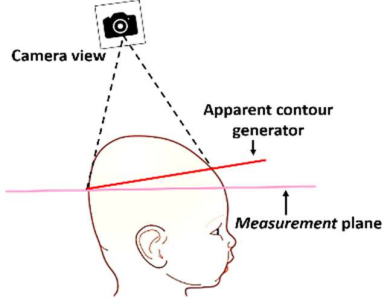


**Figure 2.** Different apparent contour generators can lead to different top-view photos.

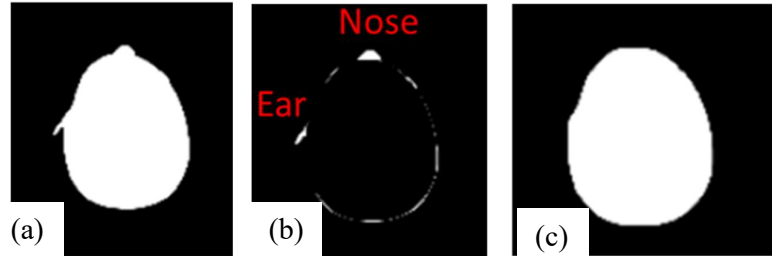


**Figure 3.** Extraction of the head contour: a) top view with an ear and nose visible, b) automatic detection of the nose and the ear, c) the final head contour used to compute the shape.

To reduce the variability in measurement from different camera angles and positions, we used multiple frames at random angles, and combined the results. We observed that the effect of novice user input can be substantially reduced using this method that analyzes multiple data points from each user, thus increasing the accuracy of the computation of cranial shape parameters used for the clinical evaluation of DPB. We then compared *CI* and *CVAI* computed from angles selected by an expert user with those from “novice users”—one image selected at random angle and distance within the defined ranges, and with “our method”—combination of 5 or 10 images selected at randomly distributed angles and distances. We also evaluated how these methods perform for the detection and classification of DPB.

### 3. RESULTS

**Accuracy of photograph-based method in the absence of user variability.** The Spearman correlation coefficients between our method and the ground-truth 3D measurements were 0.94 ( $p < 0.001$ ), and 0.96 ( $p < 0.001$ ) for *CI* and *CVAI*, respectively (Figure 4).

**Effect and compensation of variation in camera angle and distance on *CI* and *CVAI*.** Figure 5 shows an example of the effect of the variability in camera angle and distance. The *CI* error range was  $[-6.0, 2.0]$ , and the *CVAI* error range was  $[-5.0, 5.0]$ . The *CI* typical range is  $[65, 105]$ , and the *CVAI* typical range is  $[-23, 23]$ . Although this large variation in simulated camera parameters may be exaggerated, the range of errors can result in incorrect diagnosis, and

classification of severity of DPB. In general, the effect of the camera distance from the head was more pronounced on *CI* than *CVAI* while the effect of the roll angular error was more evident on *CVAI* than *CI*.

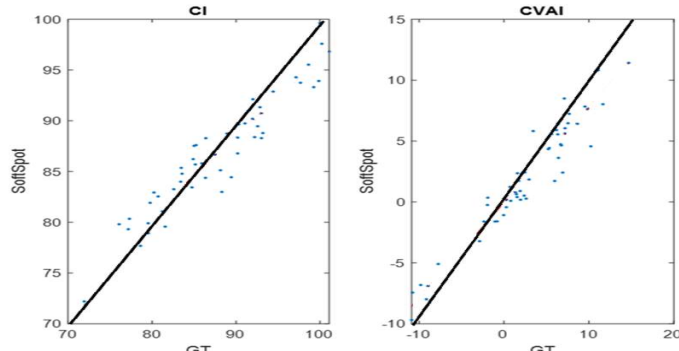


**Figure 4.** Results of regression analysis comparing results from *SoftSpot* to those of ground-truth using a least square linear regression (red line). Black line shows the ideal scenario (zero error).

Table 1 shows results when we further process the data acquired by novice users. These findings suggest that our approach based on combining the results from multiple pictures substantially reduces the error. The proposed methods to compensate for these errors improved the limits of agreement within the 95% of confidence interval in the Bland-Altman plot analysis for *CI* and *CVAI* to [-0.5,3.0], and [-1.3,1.6] respectively (Table 1 and Figure 6).

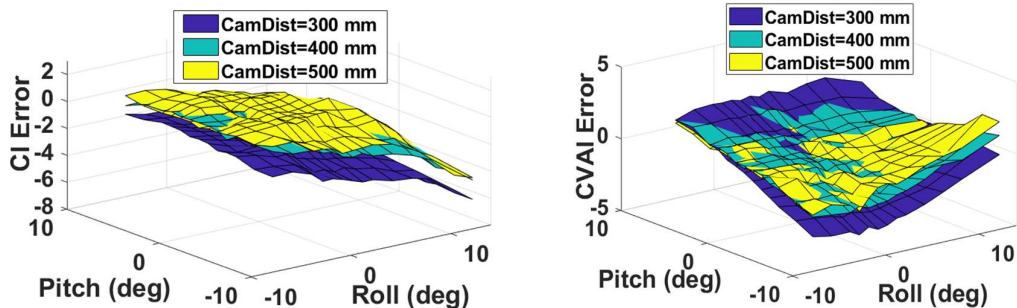


**Figure 5.** User input variables from camera distance and angle: (left) the effect on *CI*; (right) the effect on *CVAI*.

**Table 1.** Results of compensation for the effect of camera angle and distance demonstrated by the limits of agreement (LoA) in the Bland-Altman test.

	LoA in <i>CI</i>	LoA in <i>CVAI</i>
A random picture	[-3.6, 5.3]	[-3.6, 4.2]
Our method (5 random angle)	[-0.9, 3.2]	[-1.4, 1.6]
Our Method (10 random angles)	[-0.5, 3.0]	[-1.3, 1.6]

**DPB detection and classification.** Using the datasets of DPB and normal cases, we compared the ground-truth with the DPB detection, and classification results of *SoftSpot* after eliminating the effect of camera angle and distance. As shown in Table 2, *SoftSpot* was able to successfully detect all DPB cases (100% accuracy) using the combination of *CI* and *CVAI*. Table 3 shows the confusion matrix for the classification of type of DPB indicating that our approach can accurately detect DPB and indicate the type of condition.

Table 2. Evaluation of <i>SoSSpot</i> DPB detection.			
	CI	CVAI	Combined
Accuracy	96%	96%	100%
Sensitivity	100%	94%	100%
Specificity	85%	100%	100%

#### 4. CONCLUSIONS

In this study, we developed algorithms that can accurately assess the presence of DPB from top-view pictures of infant heads. We quantified the effect of the user variability including camera angle, and the distance from the head. To compensate for the camera angle/distance, we used multiple measurements from different angles to substantially reduce the errors. Our results with retrospective 3D data showed 100% accuracy for the detection of DPB, and prove the feasibility of our approach for the classification of types of DPB. Future studies will be performed with larger and prospective data.

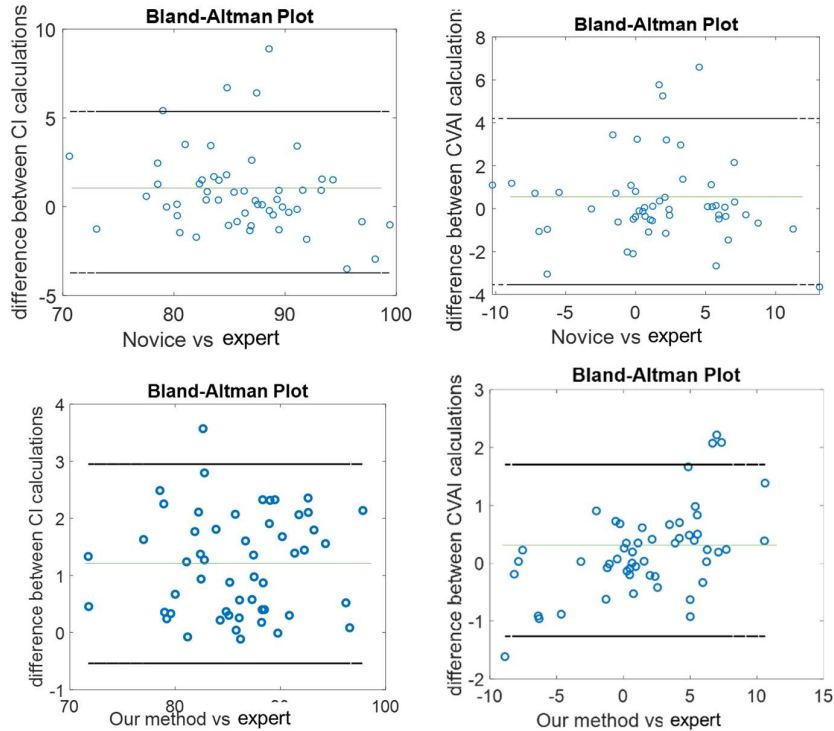


**Figure 6.** Bland Altman plot comparing our method, and the novice user with the expert user. Black lines show limits of agreements and green line shows the bias. Notable improvement in the limits of agreement can be seen with our method.

**Table 3.** Confusion matrix for the classification of type of DPB using *SoSSpot*.

		Brachycephaly	Schaphocephaly	Normal
CI	Brachycephaly	40	0	0
	Schaphocephaly	0	2	0
	Normal	2	0	9
CVAI	Right plagioccephaly	Left plagioccephaly	Normal	
	Right plagioccephaly	22	0	2
	Left plagioccephaly	0	7	0
	Normal	0	0	22

**Acknowledgement.** This work was supported by the National Science Foundation SBIR Phase I award No. 1914051.

## References

1. A. Mawji, et al., "The incidence of positional plagiocephaly: a cohort study,". *Pediatrics*. 2013;3438.
2. 2 IY. Moon, et al., "Analysis of Facial Asymmetry in Deformational Plagiocephaly Using Three-Dimensional Computed Tomographic Review," *Archives of craniofacial surgery*, " 2014;15(3):109-16.
3. BR. Collett, et al., "Development in toddlers with and without deformational plagiocephaly," *Arch Pediatr Adolesc Med*. 2011;165(7):653-8.
4. ML. Speltz, et al., "Case-control study of neurodevelopment in deformational plagiocephaly," *Pediatrics*. 2010;0052.
5. BR. Collett, et al., "Development at age 36 months in children with deformational plagiocephaly," *Pediatrics*. 2013;131(1):e115.
6. BL. Hutchison, et al., "Serial developmental assessments in infants with deformational plagiocephaly," *J Pediatric Child Health*. 2012;48(3):274-8.
7. RK. Kordesani, et al., "Neurodevelopmental delays in children with deformational plagiocephaly," *J Plastic Reconstructive Surgery*. 2006;117(1):207-18.
8. E. Courchesne, et al., "Evidence of brain overgrowth in the first year of life in autism," *JAMA*. 2003;290(3):337-44.
9. LM. Elder et al., "Head circumference as an early predictor of autism symptoms in younger siblings of children with autism spectrum disorder," *J autism and developmental disorders*. 2008 ;38(6):1104-11.
10. E. Fombonne, et al., "Microcephaly and macrocephaly in autism" *J autism and developmental disorders*. 1999;29(2):113-9.
11. SM. Zahl, et al., "Routine measurement of head circumference as a tool for detecting intracranial expansion in infants: what is the gain? A nationwide survey. *Pediatrics*. 2008 Mar 1;121(3):e416-20.
12. M. Seruya et al., "Total cranial vault remodeling for isolated sagittal synostosis: part I. Postoperative cranial suture patency," *J Plastic Reconstructive Surgery*, 2013;132(4):610e.
13. DR. Bronfin, "Misshapen heads in babies: position or pathology?," *The Ochsner Journal*. 2001 Oct;3(4):191-9.
14. GH. Noritz, et al., "Motor delays: early identification and evaluation," *Pediatrics*. 2013 May 27:peds-2013.
15. L. Zwaigenbaum et al., "Early identification and interventions for autism spectrum disorder: executive summary," *Pediatrics*. 2015 Oct 1;136(Supplement 1):S1-9.
16. Top 6 benefits of early diagnosis in kids; available at <http://www.kidsfirstraleigh.com/top-6-benefits-of-early-diagnosisscreening-tools/>. Accessed 12/1/2018.
17. 17 A. Ritter, "Positional Plagiocephaly: Prevention is Key," *AAP Grand Rounds*. 2014;32(2):24.
18. SA. Gaetani, "A pediatric epidemic: Deformational plagiocephaly/brachycephaly and congenital muscular torticollis," *Pediatrics*, 36(2).
19. J. Carson, et al., "Craniometer. Instruments of Science: An Historical Encyclopedia". *Taylor & Francis*, 1998, (2)157-9.
20. Digital Surface Imaging (DSi) system [Internet], Crainal Technologies Inc., Available from: <http://www.cranialtech.com/treatment/doc-experience>.
21. H. Schaaf, et al., "Accuracy of photographic assessment compared with standard anthropometric measurements in nonsynostotic cranial deformities," *The Cleft Palate-Craniofacial Journal*. 2010;47(5):447-53.
22. EN. Mortensen et al., "Interactive segmentation with intelligent scissors," *Graphical Models Image Process*. 1998;60(5):349-84.
23. EN. Mortensen, et al., "Intelligent scissors for image composition," *Proceedings of the 22nd annual conference on Computer graphics and interactive techniques ; ACM*; 1995
24. EW. Dijkstra. "A note on two problems in connexion with graphs," *Numerische mathematik*. 1959;1(1):269-71.
25. W. Gonzalez, et al., "Digital image processing using MATLAB," Third, New Jersey: Prentice Hall. 2004.
26. J. Sato, et al., "Affine reconstruction of curved surfaces from uncalibrated views of apparent contours," *IEEE transactions on pattern analysis and machine intelligence*, 21(11), pp.1188-1198.